Organization of talin and vinculin in adhesion plaques of wet-cleaved chicken embryo fibroblasts

CONSTANCE A. FELTKAMP*, MARIAN A. P. PIJNENBURG and ED ROOS

Division of Cell Biology, The Netherlands Cancer Institute (Antoni van Leeuwenhoek Huis), Plesmanlaan 121, 1066 CX Amsterdam, The Netherlands

* Author for correspondence

Summary

We have studied the fine structure of adhesion plaques in chicken embryo fibroblasts (CEF) and visualized the localization of vinculin and talin using immunoelectron microscopy on CEF opened by 'wet-cleaving'. This procedure, performed with nitrocellulose on cells grown on electron microscope grids, cleaved the CEF close to the inner face of the ventral membrane or at a slightly higher level through the cytoplasm. In the resulting preparations, adhesion plaques were identified by their localization at the end of microfilament bundles and by their density of vinculin and talin. The plaques showed a substructure of moderately electron-dense parallel bands that were interconnected. Both the parallel bands as well as the interconnecting threads showed a high density of vinculin and talin labels, whereas neither the surrounding membrane cytoskeleton nor the overlaying bundled microfilaments were labeled. In stereomicrographs, we observed no difference between the distances from vinculin or talin label, respectively, to the plasma membrane. In early spreading cells, vinculin and talin were found to be deposited simultaneously in fine radiating streaks that covered rather large parts of the ventral membrane at areas of close contact with the substratum. These streaks, which were initially overlayed by an isotropic cytoskeletal network without filament bundles, were the apparent precursors of later formed adhesion plaques. These observations suggest that there are no separate layers of talin and vinculin, but rather that adhesion plaques consist of a dense network of talin and vinculin. The observations strongly support the model proposed by Bendori *et al.* (1989), *J. Cell Biol.* 108, 2383–2393, that was based on the location of vinculin- and talin-binding sites in the vinculin molecule.

Key words: adhesion plaques, immunoelectron microscopy, talin, vinculin.

Introduction

Adhesion between fibroblasts and a solid substratum is provided for by adhesion plaques, domains in the ventral membrane to which bundled actin filaments are anchored and where the distance between cell surface and substratum is minimal. Adhesion plaques contain concentrations of transmembrane integrins that bind to extracellular matrix molecules and, at the cytoplasmic face of the membrane, proteins that are supposed to form part of a chain linking actin filaments to the membrane (for reviews see Geiger *et al.* 1987; Burridge *et al.* 1988). *In vitro* studies have demonstrated that talin binds both to the cytoplasmic part of integrin (Horwitz *et al.* 1986) and to vinculin (Burridge and Mangeat, 1984), which in turn is able to bind α-actinin (Otto, 1983; Wilkins *et al.* 1983; Wachstock *et al.* 1987), an actin-binding protein. Moreover, self-association of vinculin (Molony and Burridge, 1985; Milan, 1985) and direct insertion of vinculin in the plasma membrane (Niggli *et al.* 1986) have been described. Recently, an interaction between α-actinin and the β_1 integrin subunit was also found (Otey *et al.* 1990). These interactions, together with the presence in adhesion plaques of other proteins for which a structural function has been proposed (Beckerle, 1986; Turner *et al.* 1990), indicate that the adhesion plaque is a more complex structure than was previously thought.

On the basis of molecular interactions and morphological data, models of the adhesion plaque have been proposed (Geiger *et al.* 1987; Burridge *et al.* 1988). Most morphological studies on adhesion plaques have been performed with immunofluorescence, demonstrating the presence and relative concentration of specific components, the kinetics of their redistribution during formation of adhesion plaques (Geiger *et al.* 1984; DePasquale and Izzard, 1987; Izzard, 1988; Rinnerthaler *et al.* 1988) and their disappearance as induced by transforming viruses or growth factors (Boschek *et al.* 1981; David-Pfeuty and Singer, 1980; Herman and Pledger, 1985; Brands *et al.* 1990). Immunoelectron microscopic studies give more detailed information on the localization of adhesion plaque molecules (Geiger *et al.* 1980; Chen and Singer, 1982; Nicol and Nermut, 1987; Brands *et al.* 1990; Semich and Robenek, 1990). They are, however, scarce, probably due to technical difficulties.

Recently, we have demonstrated that the 'wet-cleaving' technique allows for easy access of macromolecules to the cytoplasmic surface of the ventral plasma membrane (Brands and Feltkamp, 1988). Using this method we now show that at adhesion plaques, where bundled actin

filaments terminate, vinculin and talin are concentrated at equal distances from the membrane in a thin layer with a specific substructure. In early spreading cells, larger areas of close contact with the substratum are occupied by a comparable layer. Here, however, no major rearrangement of the actin filamentous network was induced.

Materials and methods

Cells

Primary normal chicken embryo fibroblasts (CEF), prepared from day-11 embryos, were grown in Dulbecco's modified Eagle's medium (DMEM, Gibco) containing 10% fetal calf serum and 100 units penicillin/streptomycin per ml, and were used between passages 3 and 8.

Antibodies

Immunopurified rabbit polyclonal antibodies against vinculin and talin have been described previously (Brands and Feltkamp, 1988; Brands *et al.* 1990). For double labeling, mouse monoclonal anti-vinculin antibody (BioMakor, Rehovot, Israel) was used. As secondary antibodies we used goat anti-rabbit IgG (GAR) and goat anti-mouse IgG (GAM) conjugated to 5 nm or 10 nm gold particles (Janssen Pharmaceutica, Beerse, Belgium), or conjugated to fluorescein isothiocyanate (FITC) or tetramethylrhodamine isothiocyanate (TRITC) (Nordic Pharmaceutical, Tilburg, The Netherlands). Affinity-purified rabbit polyclonal antibodies against tubuline were kindly provided by Drs J. de Mey and M. de Brabander (Janssen Pharmaceutica, Beerse, Belgium).

Wet and dry cleaving

Wet cleaving was essentially performed according to Brands and Feltkamp (1988). CEF were grown on Formvar/carbon-covered nickel EM grids and used between 15 min and 24 h after seeding. After a short rinse in PBS, the cells were overlayed with a piece of moistened nitrocellulose paper and cleaved by lifting the nitrocellulose. Generally only the ventral plasma membrane together with a thin layer of cortical material remained attached to the Formvar/carbon film. Fixation with 2% paraformaldehyde (PF) or with a mixture of 2% PF and 0.01% glutaraldehyde (GA) in a cytoskeleton-stabilizing buffer containing 60 mM Pipes, 25 mM Hepes, 10 mM EGTA and 2 mM $MgCl_2$, pH 6.9 (PHEM) or in PBS was performed either before or after cleavage, as will be indicated. Dry cleaving was essentially performed according to Mesland and Spiele (1983). The fixation procedure was similar to that used for wet cleaving. Critical-point-dried cells were cleaved by means of a piece of Scotch adhesive tape.

Immunofluorescence

CEF, cultured on glass coverslips, were rinsed with PBS, fixed with 2% PF and permeabilized by a 1 min incubation with 0.1% Triton X-100. Immune incubations were performed at room temperature for 30–90 min, the antibodies were diluted with PBS containing 1% bovine serum albumine. Generally the FITC-labeled secondary antibodies were mixed with TRITC-labeled phalloidin (Molecular Probes Inc., Eugene, OR) in order to counterstain filamentous actin (F-actin). Cells grown on glass were also studied with interference-reflection microscopy (IRM) with the Zeiss antiflex system (using an Antiflex 63/1.25 oil immersion objective). In parallel with immunoelectron microscopic experiments, immunofluorescence was performed on wet-cleaved cells grown on EM grids.

Immunoelectron microscopy

When necessary, immune incubations were preceded by an incubation with 0.02 M glycine in order to quench free aldehyde groups. Wet-cleaved cells, fixed before or after cleaving, were immunolabeled with antibodies against vinculin, talin or tubulin for 90 min at room temperature, followed after thorough rinsing by a 60 min incubation with the corresponding gold-labeled secondary antiserum. For double labeling, the first incubation contained a mixture of mAb anti-vinculin and polyclonal anti-talin antibodies, and the second incubation anti-mouse and anti-goat antibodies labeled with gold particles of different size (5 nm and 10 nm). After thorough rinsing, the cells were postfixed with 0.1% GA for 15 min at room temperature and 0.1% OsO_4 for 5 min at 4°C, stained with uranyl acetate, dehydrated in a series of ethanol and critical point dried. Great care was taken to dry the ethanol used for the last dehydration step and the liquid CO_2 used for critical point drying. The grids were immediately viewed in a Philips EM 301 electron microscope, or stored for short periods in a dry environment. Stereomicrographs were taken at a tilt angle of ±6°.

Decoration of actin filaments

Wet-cleaved preparations of unfixed cells were incubated for 5 min in a 1–2 mg ml^{-1} solution of heavy meromyosin (HMM) or its S_1 fragment (both from Sigma Chemical Co., St Louis, MD) and further processed according routine methods. A tannic acid treatment (0.1%, 15 min) was included between GA and OsO_4 fixation.

Results

Adhesion plaques in spread cells

From 1 h after plating, most cells were spread over the substratum and polarized. In such cells, adhesion plaques were identified by immunofluorescence after Triton X-100 permeabilization as distinct concentrations of talin and vinculin at the end of bundled actin filaments (Fig. 1). In IRM they were visible as very dark reflecting areas (Fig. 1C). Immunofluorescence on wet-cleaved cells spread on Formvar-coated EM grids showed a similar distribution of vinculin and talin to that in permeabilized cells (Fig. 2A,B). After cleavage, the presence and length of F-actin bundles depended on the level of the cleavage plane. Filament bundles sometimes fully covered the ventral membrane (Figs 2C, 3A), but were usually removed by cleavage. In the latter case, a thin layer of parallel filaments remained only locally attached to the membrane (Fig. 3B). These areas resembled vinculin- and talin-positive adhesion plaques, as seen by immunofluorescence, in localization, size and shape. When cleavage was very deep, a seemingly bare plasma membrane remained attached to the EM grid.

Immunoelectron microscopy of talin and vinculin

The distribution of talin and vinculin was studied by incubating wet-cleaved cells with specific antibodies and a gold-conjugated secondary antibody.

Vinculin- and talin-positive domains were found to be localized at the end of filament bundles, which often fanned out at these adhesion plaques (Fig. 4A,B). The size of the domains varied from one to several μm in length and 0.05–1 μm in width, similar to that of adhesion plaques seen in immunofluorescence. Outside the plaques only few gold particles were observed.

No major differences were observed in number and distribution of gold particles between specimens that were PF-fixed before and those fixed after cleaving. However, in the former the fine morphology was better preserved. In stereomicrographs it was particularly evident that filaments and organelles such as vesicles were not labeled. This shows that the reaction with vinculin and talin is specific and, moreover, that no vinculin or talin is attached by fixation or during critical-point drying to filaments or other structures.

The density of the gold label depended on the position of

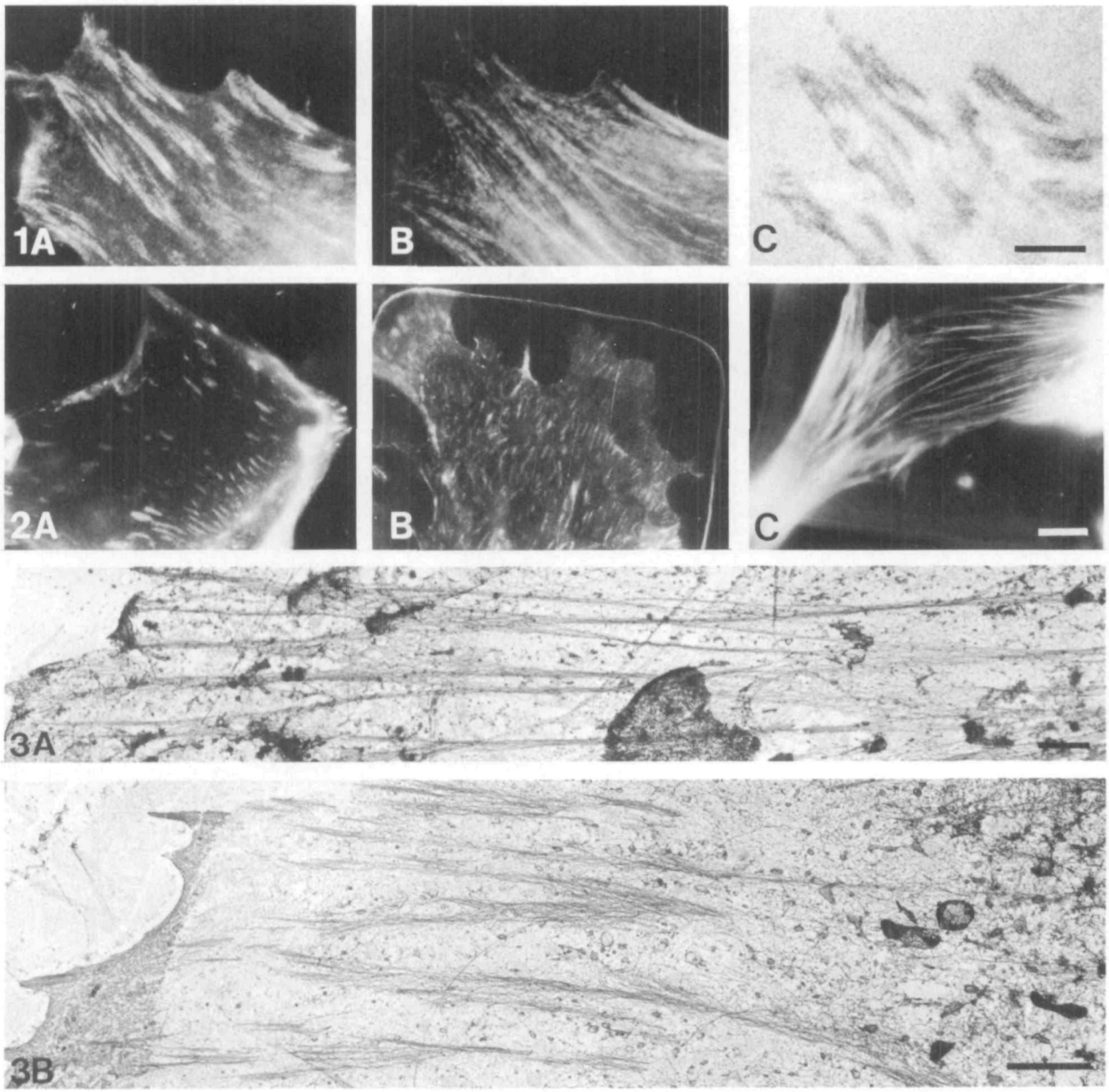

Fig. 1. Distribution of talin (A) and F-actin (B) in a TX-100-permeabilized CEF, 4 h after seeding on glass. (C) Interference reflection of the same cell. Bar, 10 μm.
Fig. 2. Distribution of vinculin (A), talin (B) and F-actin (C) in wet-cleaved CEF, 2 h after seeding on EM grids. Bar, 10 μm.
Fig. 3. Dry-cleaved CEF grown on EM grids for 24 h (A) and 2 h (B). When the plane of cleavage is relatively high (A), bundled filaments remain attached to the ventral membrane. In deeper-cleaved cells (B), filaments remain attached at areas that resemble adhesion plaques in location, size and shape. Bars, 2 μm.

the plane of cleavage. When (parts of) the filamentous network remained attached to adhesion plaques, fewer gold particles were detected than in deep-cleaved preparations, probably due to reduced accessibility.

The nature of the filaments was studied by decoration with heavy meromyosin (HMM) or its S_1 fragment. Practically all filaments attached to the ventral membrane were decorated and thus consisted of actin (Fig. 5). Some isolated intermediate filaments, as well as short filaments perpendicular to and attached to bundled actin filaments were not decorated. The twisted-rope shape of the decoration was best seen in replicas prepared from wet-cleaved cells grown on glass (Fig. 5B). After decoration of filaments by HMM or S_1, which has to be performed before fixation, the number of filaments attached to the membrane decreased. Moreover, decoration induced a straighter configuration of the filaments. This is in agreement with observations of Bennet and Condeelis (1984).

Fine structure of adhesion plaques

The talin- and vinculin-labeling gold particles were not randomly distributed within the domain of the adhesion plaque. Especially in larger plaques, they were organized in several parallel interconnected bands (Fig. 6A,B,C).

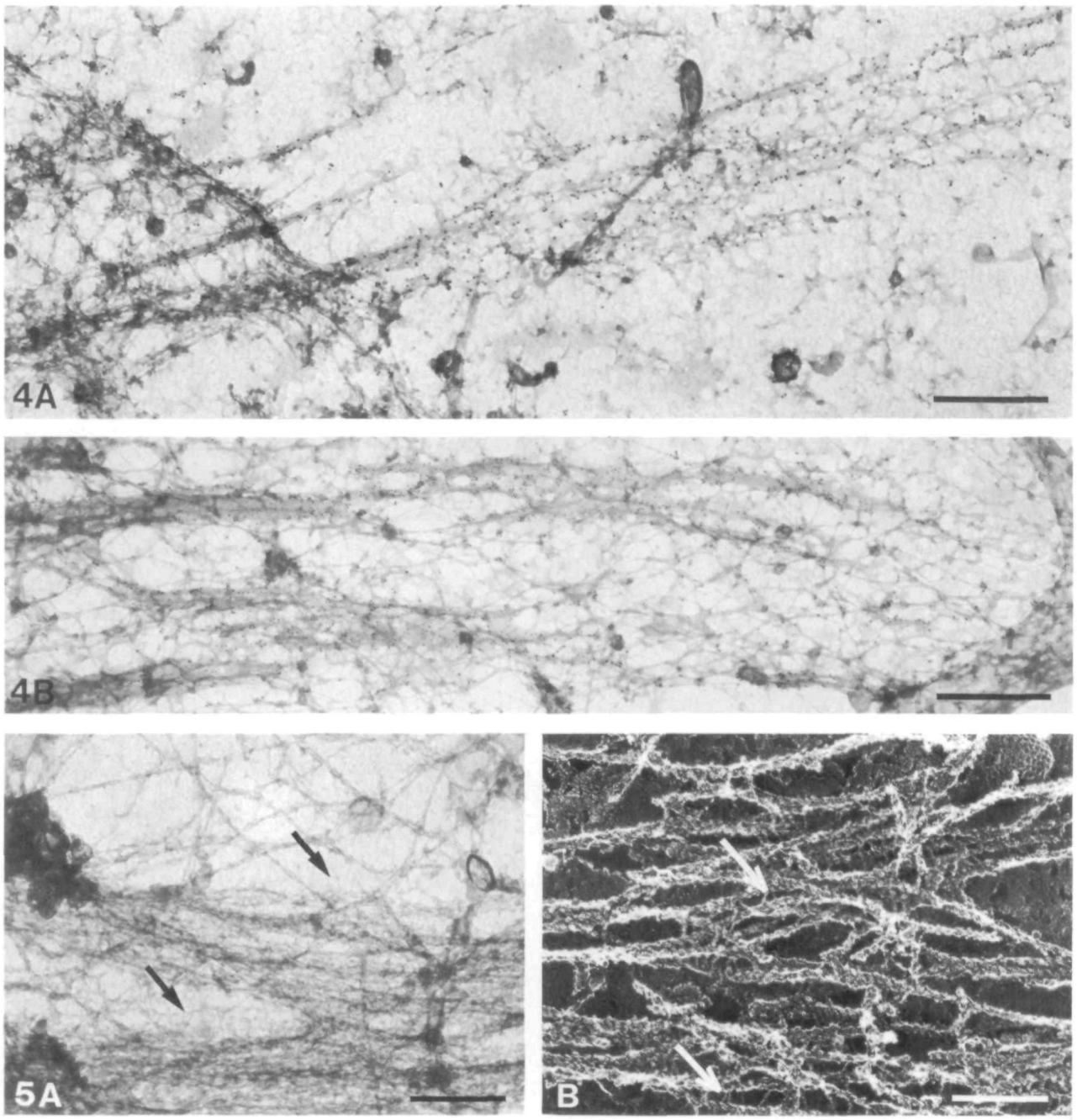

Fig. 4. Distribution of vinculin (A) and talin (B) in wet-cleaved CEF grown for 2.5 h on EM grids. The cells were PF-fixed before cleavage. Vinculin is detected with mAb anti-vinculin and GAM.G10; talin with polyclonal anti-talin antibodies and GAR.G5. The gold particles are concentrated at specific domains located at the end of bundled filaments (A) and at some distance of the cell border (B). Bars, 0.5 μm.

Fig. 5. Heavy meromyosin (HMM) decoration of actin filaments. (A) CEF grown on EM grid, incubated with HMM after wet-cleaving and before fixation, dehydration and critical-point drying. (B) Replica of CEF grown on glass, treated with a mixture of HMM and 0.01 % saponin before fixation, dehydration, critical-point drying and dry-cleaving. Practically all filaments are decorated, except short filaments (arrows) perpendicular to bundled decorated filaments. Bars, 0.2 μm.

The bands, about 30–50 nm in width, followed the direction of overlaying actin filaments. Smaller plaques consisted of only one band.

In double-labeled specimens, talin- and vinculin-labeling gold particles were always fully mixed (Fig. 6B). Unfortunately, it was not possible to obtain detailed information on talin/vinculin ratios at particular sites, because the density of gold particles was highly size-dependent: label density was consistently lower with 10 nm particles, irrespective of whether they were used for detection of vinculin or talin.

In stereomicrographs, the distances between the membrane and talin label or vinculin label, respectively, were not seen to be different. High-magnification stereomicrographs showed that the parallel bands and the interconnecting threads, both tagged by gold particles, consisted of

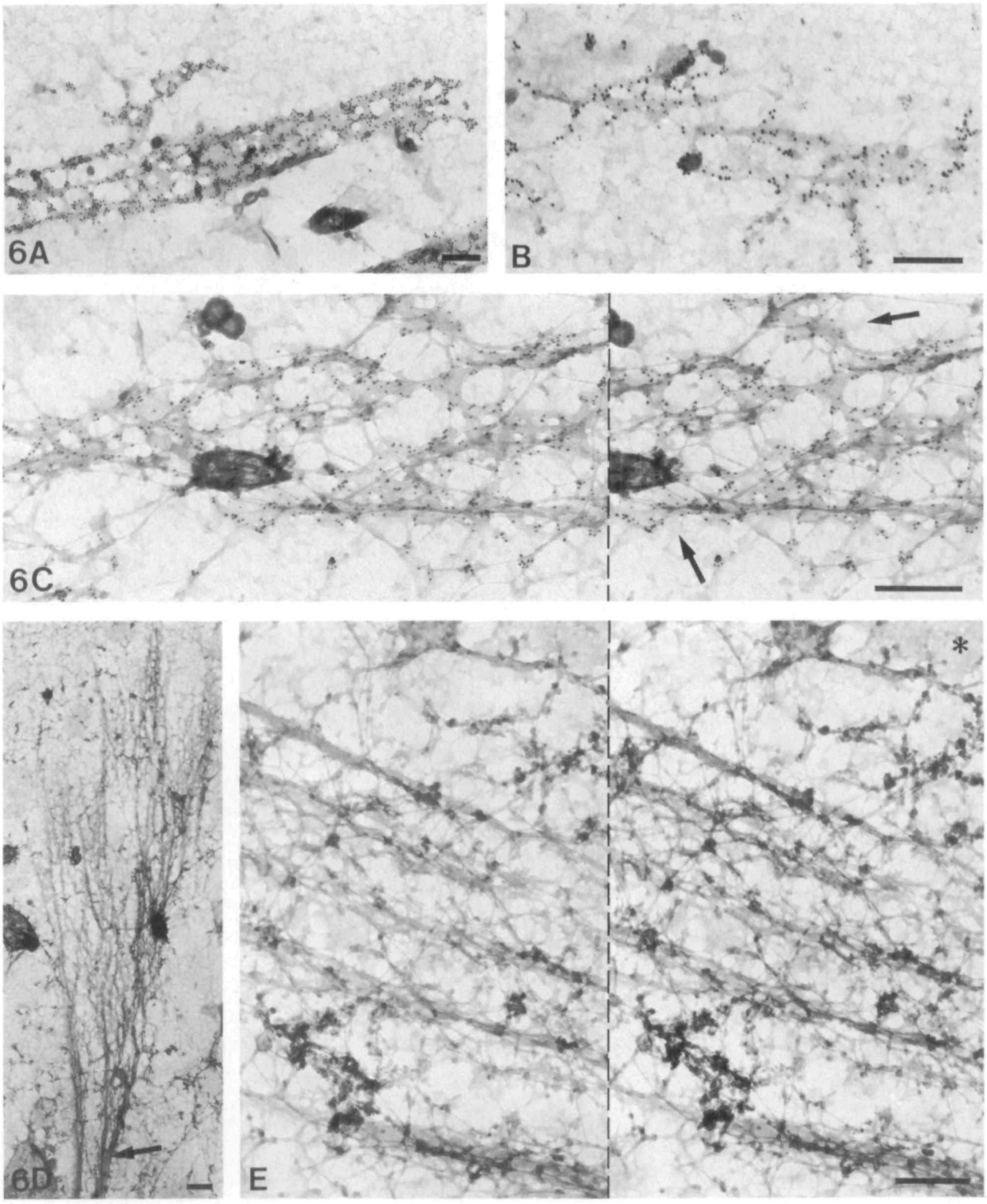

Fig. 6. CEF grown for 2 h on EM grids. (A, B, C) Wet-cleaved before immune incubations. (D, E) Dry-cleaved. Talin (A) and vinculin (C) are concentrated together (B) in domains consisting of parallel interconnected bands of relatively increased electron density. (B) Specimen double labeled for talin (10 nm gold) and vinculin (5 nm gold). (C) Stereomicrograph (right part, viewing direction from inside the cell) of a vinculin-labeled adhesion plaque shows that gold particles are localized at the thin layer of relatively electron-dense material. This layer is connected to unlabeld patches of less electron density (arrows) at the inner surface of the plasma membrane. Filaments and vesicles are not labeled. (D, E) In dry-cleaved cells a similar pattern of relatively electron-dense parallel bands is present at the end of bundled filaments (D, arrow). Stereomicrograph (E, viewing direction from inside the cell) shows that filaments closely overlay the bands. The hexagons of clathrin at a coated area (E, asterisk) indicate the level of the inner face of the plasma membrane. Bars, 0.2 μm.

a thin layer of relatively electron-dense material located close to the plasma membrane (Fig. 6C). Each band was closely overlayed by one or several actin filaments. Distinct connections between these filaments and the membrane-associated bands were rarely seen because the outermost filaments usually seemed to be embedded in the layer of relatively electron-dense material.

Outside adhesion plaques, a network of interconnected patches covered the inner surface of the plasma membrane. The electron density of these patches was lower than that of the bands in the adhesion plaques. The bands of the adhesion plaques were connected to this patchy network, as was also the layer of clathrin at coated pits (Fig. 6C,E). In contrast to the parallel arrangement at adhesion plaques, the cortical filamentous network outside the plaque was irregular or isotropic and locally connected *via* short down-pointing filaments to the patches of moderate electron density.

To exclude the possibility that the observed structure of the adhesion plaque was an artifact induced by the wet-cleaving and labeling procedures, the fine morphology of the adhesion plaque was also studied on unlabeled preparations obtained by dry-cleaving, i.e. by cleavage after critical-point drying of the cells. The fixation procedure was identical to that used in the wet-cleaving experiments (PF followed by GA and OsO_4). The fine structure of dry-cleaved adhesion plaques was not different from that in wet-cleaved immunolabeled preparations (Fig. 6D,E). Thus, the relatively high electron density of the bands in the plaques was not due to a layer of attached immunoglobulins.

Contact domains in early spreading cells

The development of adhesion plaques was studied during spreading of freshly plated cells. At the earliest stage after attachment, when most cells were still rounded, the cortical filamentous network was isotropic, and the membrane was covered only by the network of interconnected patches of moderate electron density. Only a few dispersed gold particles tagging talin or vinculin were observed.

Between 15 and 30 min after adhesion, cells spread by extension of thin lamellae often completely surrounding the cell body. Initially, the narrow space between the upper and lower membrane of the lamella was filled with an isotropic filamentous network. After further spreading, filaments were concentrically arranged at some distance from the ventral membrane, while a regular pattern of fine radiating striations covered large areas of the ventral membrane of the lamellae (Fig. 7A,C). The striations were formed by fine bands of somewhat increased electron density, 2–8 μm in length and 15–40 nm in width, with a mutual distance of 100–200 nm. The striations ended at, or at a short distance from, the outer edge of the lamellae and were seen to converge into extended microspikes. Initially, striations were overlayed by an isotropic filamentous network (Fig. 7B). Orientation parallel to striations was

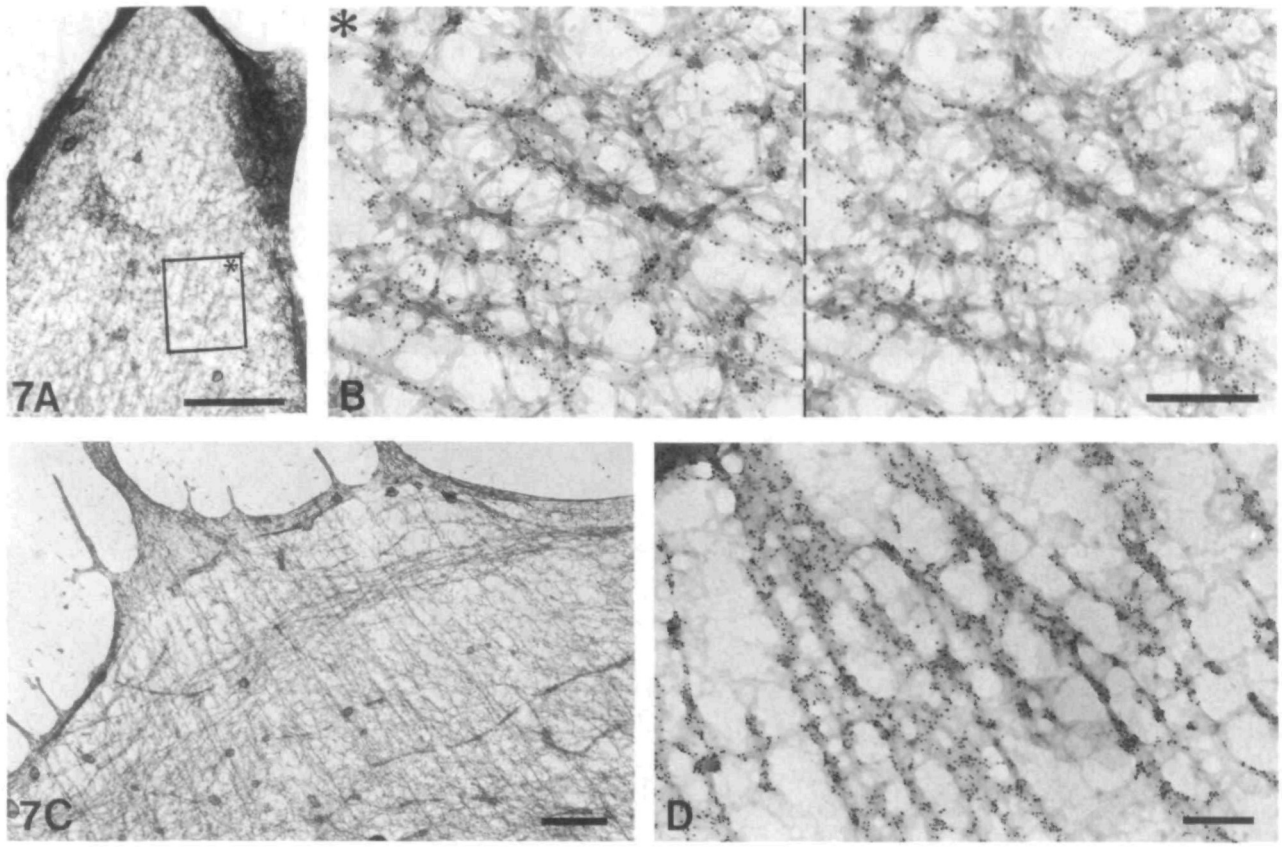

Fig. 7. CEF at 45 min (A,B), 1 h (C) and 2 h (D) after seeding on EM grids, wet-cleaved and talin-labeled (A,B,D), or dry-cleaved (C). Radiating striations cover a large area of the ventral membrane of the lamella. Overlaying filaments at first form an isotropic network (B, stereomicrograph, viewing direction from inside the cell) that is later rearranged into two directions: parallel to the striations and concentrically (C). Striations formed by talin-positive radiating bands of increased electron density cover the inner face of the membrane (B,D). Bars: 1 μm (A,C); 0.2 μm (B,D).

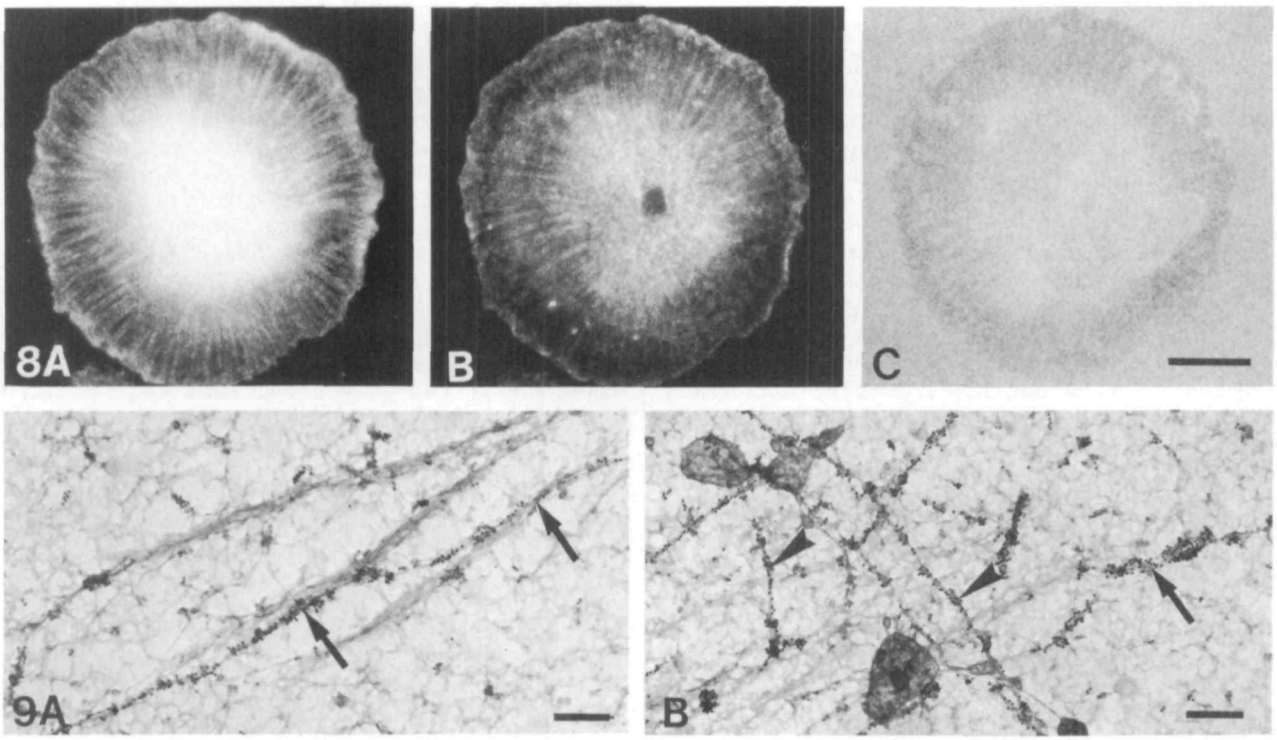

Fig. 8. Distribution of talin (A) and F-actin (B) in a Triton X-100-permeabilized CEF, 20 min after seeding on glass.
(C) Interference reflection of the same cell. Fine radiating talin-(A) and F-actin-(B) positive striations fill the lamella surrounding the cell body. The major part of the lamella is in close contact with the substratum (C). Bars, 10 μm.
Fig. 9. Distribution of tubulin in CEF, 1 h after seeding. Microtubules that remain present after wet-cleaving generally follow the direction of the bands of the adhesion plaque (A, B, arrows), but can also cross them (B, arrowheads). Bars, 0.2 μm.

only seen in the outermost filaments. At later times, more of such filaments running parallel to the striations were seen.

Talin, but practically no vinculin, was detected at the very edge of the lamellae, while both talin and vinculin were found to be concentrated in the radiating striations (Fig. 7D). With the techniques used, we could not detect a time difference between the deposition of vinculin and that of talin at the striations. Comparison of images obtained with immunofluorescence and with IRM showed that striations positive for talin, vinculin and F-actin were always localized within areas that were homogeneously grey in IRM, thus representing areas of close contact with the substratum (Fig. 8). With time, the immunofluorescence of the striations increased and darker reflecting stripes were formed within the grey area of close contact. After 30 min, distinct radiating bands of increased electron density appeared. These bands were dark in IRM, and probably represented precursor forms of adhesion plaques. They were localized at the base of finely striated areas, but also outside these areas both along the cell edge and more centrally in the cell. In the latter cases, the membrane surrounding the bands was located at a greater distance from the substratum, since it gave a very light reflection in IRM, similar to areas surrounding large fully developed adhesion plaques.

Distribution of microtubules

Comparison of fluorescent- and gold-labeled tubulin demonstrated that most microtubules were localized at some distance from the ventral membrane, and were removed or broken by cleavage. Within the cortical skeleton, most microtubules ran parallel to actin filament bundles (Fig. 9A). They were seen to overlay adhesion plaques, but in addition ran also between them and could cross filament bundles (Fig. 9B). In early spreading cells microtubules followed three main patterns: radiating, parallel to the outer edge of the lamella, and (more centrally in the cell) concentric and embedded in the mass of concentric filaments. The mutual distance between radiating microtubules was larger than that of the fine striations.

Discussion

To study the fine structure of adhesion plaques and the localization of its components with (immuno)electron microscopy, it is of importance to keep both the ventral plasma membrane and the cortical part of the cytoskeleton intact. Moreover, the latter has to be sufficiently thin to allow for penetration of gold-labeled antibodies. This is possible when cells are cleaved prior to immunolabeling, as has been demonstrated by Nicol and Nermut (1987), Brands *et al.* (1990), and Semich and Robenek (1990). In the present study, cells grown on EM grids were cleaved and observed as whole mounts. Cellular material was not digested, the ventral membrane together with attached structures remained intact, and gold particles were localized in high-magnification stereomicrographs at specific structures.

In the present study we have visualized adhesion plaques in wet-cleaved fibroblasts as membrane-bound, electron-dense structures containing high levels of vinculin and talin. As is also seen by immunofluorescence, they are located at the end of microfilament bundles from which separate actin filaments were seen to terminate at these

structures. In deeply cleaved cells, the filaments and other superimposed material were removed. This improved the accessibility for immunoglobulins and gold label, since the density of vinculin and talin label was higher than in cells cleaved along higher planes. In the plaques, vinculin and talin were completely intermixed, and in stereomicrographs talin was not seen to be closer to the membrane than vinculin.

These observations are not in line with previous models of adhesion plaque structure that propose that a layer of integrin-bound talin is connected to the cytoskeleton *via* a layer of vinculin molecules. This layer in turn is connected by α-actinin, known to be located at some distance from the membrane (Chen and Singer, 1982), to actin located still further away from the membrane. More recently, a model was proposed by Bendori *et al.* (1989), based on their finding that vinculin has at least two binding sites for plaques, one for talin located in the head region, and one, in the tail region, for other vinculin molecules. The resulting network would form a dense layer at the membrane. Our present observations are fully consistent with this model. It is noteworthy that our results are in agreement with earlier observations on dense plaques in chicken gizzard muscle tissue (Volberg *et al.* 1986). Immunoelectron microscopy on frozen sections demonstrated an intermixing of vinculin and talin that was inconsistent with the models that were current at the time, but in line with the recent model of Bendori *et al.* (1989).

If this model is correct, the primary role of vinculin is likely to be the strengthening of adhesion plaques rather than linkage to the cytoskeleton. This notion is supported by our previous observations on morphological transformation induced by temperature shift in chicken fibroblasts infected with temperature-sensitive RSV (Brands *et al.* 1990). Vinculin was seen to be rapidly lost, and adhesion plaques connected to actin filaments, with practically no vinculin present, were seen to exist transiently. A similar rapid disappearance of vinculin from otherwise seemingly intact adhesion plaques was earlier found by Herman and Pledger (1985) after PDGF treatment. Furthermore, Ben-Ze'ev *et al.* (1990) have found that under certain conditions fibroblasts spread and adhere to a substratum without concentration of vinculin into plaques.

It remains unclear how the vinculin-talin layer is connected to the cytoskeleton. The observations by Bendori *et al.* (1989) suggest that, apart from the above-mentioned binding sites, vinculin also has a site interacting with the cytoskeleton. In the present study, we have seen terminating individual actin filaments apparently embedded within the adhesion plaque. It is therefore possible that vinculin does play a role in binding of actin filaments, possibly through its interaction with α-actinin or *via* paxillin (Turner *et al.* 1990). Given the existence of vinculin-deficient plaques, however, other proteins should also be involved, and are likely to be more important.

Our results show that fully developed, large adhesion plaques are not homogeneous, but consist predominantly of parallel bands, interconnected by threads of apparently the same dense vinculin–talin network. The bands run parallel to the overlaying filaments, suggesting that a mutual interaction determines their direction. Singer *et al.* (1989) observed a similar substructure at the outer ventral surface of adhesion plaques. It seems therefore likely that other plaque components, such as the transmembrane integrins, are also concentrated in the bands, but this remains to be established.

Adhesion plaques were connected to the surrounding membrane-associated network, that consists of moderately electron-dense patches at the level of the membrane, overlayed by and connected to an isotropic cortical filament network. In a previous study, we have shown that concanavalin A-binding glycoproteins are located at the patches (Roos *et al.* 1985). Therefore, their electron density is probably due to concentration of transmembrane molecules. In suspended fibroblasts, as in most cells in suspension (Mesland and Spiele, 1983), this is the only form of cortical network present.

Formation of adhesion plaques is preceded by adhesion of the cells to the substratum and formation of areas of close contact. In these areas, talin and vinculin are recruited from the cytoplasm and incorporated at the membrane into fine radiating striations. We did not observe a stage at which talin, but no vinculin, was present in the striations. Early striations were seen to be connected to one or very few actin filaments that follow their direction, the overlaying network remained isotropic. These filaments could be responsible for the formation and direction of vinculin and talin concentrations, as is suggested by Izzard and Lochner (1980). However, in general no major reorganization of the filamentous network overlaying striations was detected. Therefore, the possibility cannot be ruled out that integrin clustering into a specific pattern (Segal *et al.* 1983) may precede concentration of talin and vinculin and determine the direction of the actin filaments, consistent with the findings of Dejana *et al.* (1988). Since the time interval between redistribution of actin and linking molecules is very short (DePasquale and Izzard, 1987), the chance to detect the sequence of reorganization of the different components with our methods is very small. Hence, we cannot establish whether talin binds first to the plaque sites or whether talin and vinculin simultaneously assemble at these sites.

Since, with time, some striations broadened while their interspace increased, it seems probable that these are precursor forms of adhesion plaques.

The distribution of microtubules indicates that they are primarily involved in formation of the leading lamellae and in determination of their direction, and less in formation of adhesion plaques.

The authors thank Harry van Drimmelen for technical assistance with the production of polyclonal antisera, J. De Mey and M. De Brabander for supply of polyclonal anti-tubulin antibodies, and Nico Ong for excellent photographic work.

References

Beckerle, M. C. (1986). Identification of a new protein localized at sites of cell–substrate adhesion. *J. Cell Biol.* **103**, 1679–1687.

Bendori, R., Salomon, D. and Geiger, B. (1989). Identification of two distinct functional domains on vinculin involved in its association with focal contacts. *J. Cell Biol.* **108**, 2383–2393.

Bennet, H. and Condeelis, J. (1984). Decoration with myosin subfragment-1 disrupts contacts between microfilaments and the cell membrane in isolated *Dictyostelium* cortices. *J. Cell Biol.* **99**, 1434–1440.

Ben-Ze'ev, A., Reiss, R., Bendori, R. and Gorodecki, B. (1990). Transient induction of vinculin gene expression in 3T3 fibroblasts stimulated by serum growth factors. *Cell Regln* **1**, 621–636.

Boschek, C. B., Jockusch, B. M., Friis, R. R., Back, R., Grundmann, E. and Bauer, H. (1981). Early changes in the distribution and organization of microfilament proteins during cell transformation. *Cell* **24**, 175–184.

Brands, R., De Boer, A., Feltkamp, C. A. and Roos, E. (1990). Disintegration of adhesion plaques in chicken embryo fibroblasts upon

Rous sarcoma virus-induced transformation: different dissociation rates for talin and vinculin. *Expl Cell Res.* **186**, 138–148.
BRANDS, R. AND FELTKAMP, C. A. (1988). Wet cleaving of cells: a method to introduce macromolecules into the cytoplasm. *Expl Cell Res.* **176**, 309–318.
BURRIDGE, K., FATH, K., KELLY, T., NUCKOLLS, G. AND TURNER, C. (1988). Focal adhesions: transmembrane junctions between the extracellular matrix and the cytoskeleton. *A. Rev. Cell Biol.* **4**, 487–525.
BURRIDGE, K. AND MANGEAT, P. (1984). An interaction between vinculin and talin. *Nature* **308**, 744–745.
CHEN, W.-T. AND SINGER, S. J. (1982). Immunoelectron microscopic studies of the sites of cell–substratum and cell–cell contacts in cultured fibroblasts. *J. Cell Biol.* **95**, 205–222.
DAVID-PFEUTY, T. AND SINGER, S. J. (1980). Altered distributions of the cytoskeletal proteins vinculin and α-actinin in cultured fibroblasts transformed by Rous sarcoma virus. *Proc. natn. Acad. Sci. U.S.A.* **77**, 6687–6691.
DEJANA, E., COLELLA, S., CONFORTI, G., ABBADINI, M., GABOLI, M. AND MARCHISIO, P. C. (1988). Fibronectin and vitronectin regulate the organization of their respective Arg-Gly-Asp adhesion receptors in cultured human endothelial cell. *J. Cell Biol.* **107**, 1215–1223.
DEPASQUALE, J. A. AND IZZARD, C. S. (1987). Evidence for an actin-containing cytoplasmic precursor of the focal contact and the timing of incorporation of vinculin at the focal contact. *J. Cell Biol.* **105**, 2803–2809.
GEIGER, B., AVNUR, Z., RINNERTHALER, G., HINSSEN, H. AND SMALL, J. V. (1984). Microfilament-organizing centers in areas of cell contact: cytoskeletal interactions during cell attachment and locomotion. *J. Cell Biol.* **99**, 83s–91s.
GEIGER, B., TOKUYASU, K. T., DUTTON, A. H. AND SINGER, S. J. (1980). Vinculin, an intracellular protein localized at specialized sites where microfilament bundles terminate at cell membranes. *Proc. natn. Acad. Sci. U.S.A.* **77**, 4127–4131.
GEIGER, B., VOLK, T., VOLBERG, T. AND BENDORI, R. (1987). Molecular interactions in adherens-type contacts. *J. Cell Sci. Suppl.* **8**, 251–272.
HERMAN, B. AND PLEDGER, W. J. (1985). Platelet-derived growth factor induced alterations in vinculin and actin distribution in BALB/c 3T3 cells. *J. Cell Biol.* **100**, 1031–1040.
HORWITZ, A., DUGGAN, K., BUCK, C., BECKERLE, M. C. AND BURRIDGE, K. (1986). Interaction of plasma membrane fibronectin receptor with talin, a transmembrane linkage. *Nature* **320**, 531–533.
IZZARD, C. S. (1988). A precursor of the focal contact in cultured fibroblasts. *Cell Motil. Cytoskeleton* **10**, 137–142.
IZZARD, C. S. AND LOCHNER, L. R. (1980). Formation of cell-to-substrate contacts during fibroblast motility: an interference-reflexion study. *J. Cell Sci.* **42**, 81–116.
MESLAND, D. A. M. AND SPIELE, H. (1983). Plasma membrane-associated filament systems in cultured cells visualized by dry-cleaving. *J. Cell Sci.* **64**, 351–364.
MILAM, L. (1985). Electron microscopy of rotary shadowed vinculin and vinculin complexes. *J. molec. Biol.* **184**, 543–545.
MOLONY, L. AND BURRIDGE, K. (1985). Molecular shape and self association of vinculin and metavinculin. *J. Cell Biochem.* **29**, 31–36.
NICOL, A. AND NERMUT, M. V. (1987). A new type of substratum adhesion structure in NRK cells revealed by correlated interference reflection and electron microscopy. *Eur. J. Cell Biol.* **43**, 348–357.
NIGGLI, V., DIMITROV, D. P., BRUNNER, J. AND BURGER, M. M. (1986). Interaction of the cytoskeletal component vinculin with bilayer structures analyzed with a photoactivatable phospholipid. *J. biol. Chem.* **261**, 6912–6918.
OTEY, C. A., PAVALKO, F. M. AND BURRIDGE, K. (1990). An interaction between α-actinin and the β_1 integrin subunit *in vitro*. *J. Cell Biol.* **111**, 721–729.
OTTO, J. (1983). Detection of vinculin-binding proteins with an ^{125}I-vinculin overlay technique. *J. Cell Biol.* **97**, 1283–1287.
RINNERTHALER, G., GEIGER, B. AND SMALL, J. V. (1988). Contact formation during fibroblast locomotion: involvement of membrane ruffles and microtubules. *J. Cell Biol.* **106**, 747–760.
ROOS, E., SPIELE, H., FELTKAMP, C. A., HUISMAN, H., WIEGANT, F. A. C., TRAAS, J. AND MESLAND, D. A. M. (1985). Localization of cell surface glycoproteins in membrane domains associated with the underlying filament network. *J. Cell Biol.* **101**, 1817–1825.
SEGEL, L. A., VOLK, T. AND GEIGER, B. (1983). On spatial periodicity in the formation of cell adhesions to a substrate. *Cell Biophys.* **5**, 95–104.
SEMICH, R. AND ROBENEK, H. (1990). Organization of the cytoskeleton and the focal contacts of bovine aortic endothelial cells cultured on type I and III collagen. *J. Histochem. Cytochem.* **38**, 59–67.
SINGER, I. I., DAZAZAIS, D. M. AND SCOTT, S. (1989). Scanning electron microscopy of focal contacts on the substratum attachment surface of fibroblasts adherent to fibronectin. *J. Cell Sci.* **93**, 147–154.
TURNER, C. E., GLENNEY, J. R. AND BURRIDGE, K. (1990). Paxillin: a new vinculin-binding protein present in focal adhesions. *J. Cell Biol.* **111**, 1059–1068.
VOLBERG, T., SABANAY, H. AND GEIGER, B. (1986). Spacial and temporal relationships between vinculin and talin in the developing chicken gizzard smooth muscle. *Differentiation* **32**, 34–43.
WACHSTOCK, D., WILKINS, J. A. AND LIN, S. (1987). Specific interaction of vinculin with α-actinin. *Biochem. biophys. Res. Commun.* **146**, 554–560.
WILKINS, J. A., CHEN, K. Y. AND LIN, S. (1983). Detection of high molecular weight vinculin binding proteins in muscle and nonmuscle tissues with an electroblot-overlay technique. *Biochem. biophys. Res. Commun.* **116**, 1026–1032.

(Received 6 June 1991 – Accepted 13 August 1991)